# Supporting Information

## Controllable synthesis of yolk-shell-structured metal oxides with seven to ten components for finding materials with superior lithium storage properties

Seung Ho Choi,[a,b] Jung-Kul Lee,[*b] and Yun Chan Kang[*a]

[a]Department of Materials Science and Engineering, Korea University, Anam-Dong, Seongbuk-Gu, Seoul 136-713, Republic of Korea.
[b]Department of Chemical Engineering, Konkuk University, 1 Hwayang-dong, Gwangjin-gu, Seoul 143-701, Korea

*Corresponding author. Fax: (+82) 2-928-3584.(Y.C.K), Fax: (+82) 2-458-3504.(J.-K.L)

E-mail address: yckang@konkuk.ac.kr (Y.C.K), jkrhee@konkuk.ac.kr.(J.-K.L)

## Experimental Section

**Synthesis.** Multicomponent yolk-shell transition metal oxide powders with seven to ten components were prepared by a one-pot spray pyrolysis process. For simplicity, hereafter, transition metal oxides with 7, 8, 9, and 10 components will be referred to as '7-composite', '8-composite', '9-composite, and '10-composite'. The 7-composite powders contained Co, Cu, Fe, Mn, Mo, Ni, and Zn. For higher composites, Cr, W, and V components were added in order to form the 8-composite, 9-composite, and 10-composite powders. Yolk-shell metal oxide powders with complex compositions were directly prepared by spray pyrolysis from aqueous spray solutions. A schematic diagram of the ultrasonic spray pyrolysis system used to produce yolk-shell powders is shown in Scheme 1. A quartz reactor with a length of 1,200 mm and a diameter of 50 mm was used. The reactor temperature was maintained at 700 °C, and the flow rate of air used as carrier gas was 10 L $min^{-1}$. An aqueous spray solution was prepared by using inexpensive metal salts in distilled water. Detailed information about the metal salts used is provided in Table S2. Sucrose was used as the carbon source material to form the yolk-shell-structured powders. The total concentrations of metal salts and sucrose were 0.15 M and 0.7 M, respectively.

**Characterization.** The crystal structures of the multicomponent transition metal oxide powders were investigated by X-ray diffractometry (XRD; X'pert PRO MPD) using Cu K$\alpha$ radiation ($\lambda$ = 1.5418 Å). Morphological characteristics were investigated using high-resolution transmission electron microscopy (HR-TEM), (JEM-2100F), at a working voltage of 200 kV. The specific surface areas of the multicomponent transition metal oxide powders were calculated from Brunauer–Emmett–Teller (BET) analysis of nitrogen adsorption measurements (TriStar 3000).

**Electrochemical Measurements.** The capacities and cycle properties of the multicomponent transition metal oxide powders were determined using a 2032-type coin cell. The electrode was prepared from a mixture containing 70 wt% active material, 20 wt% Super P, and 10 wt% sodium carboxymethyl cellulose (CMC) binder. Lithium metal and microporous polypropylene film were used as the counter electrode and separator, respectively. The electrolyte was a 1 M $LiPF_6$ solution in a 1:1 mixture (by volume) of ethylene carbonate/dimethyl carbonate (EC/DMC) with 5% fluoroethylene carbonate. The charge/discharge characteristics of the samples were determined through cycling in the 0.001–3 V potential range at a set of fixed current densities. Cyclic voltammetry (CV) measurements were carried out at a scan rate of 0.07 mV $s^{-1}$. The size of the negative electrode was 1 cm × 1 cm and the mass loading was about 1.2 mg $cm^{-2}$.

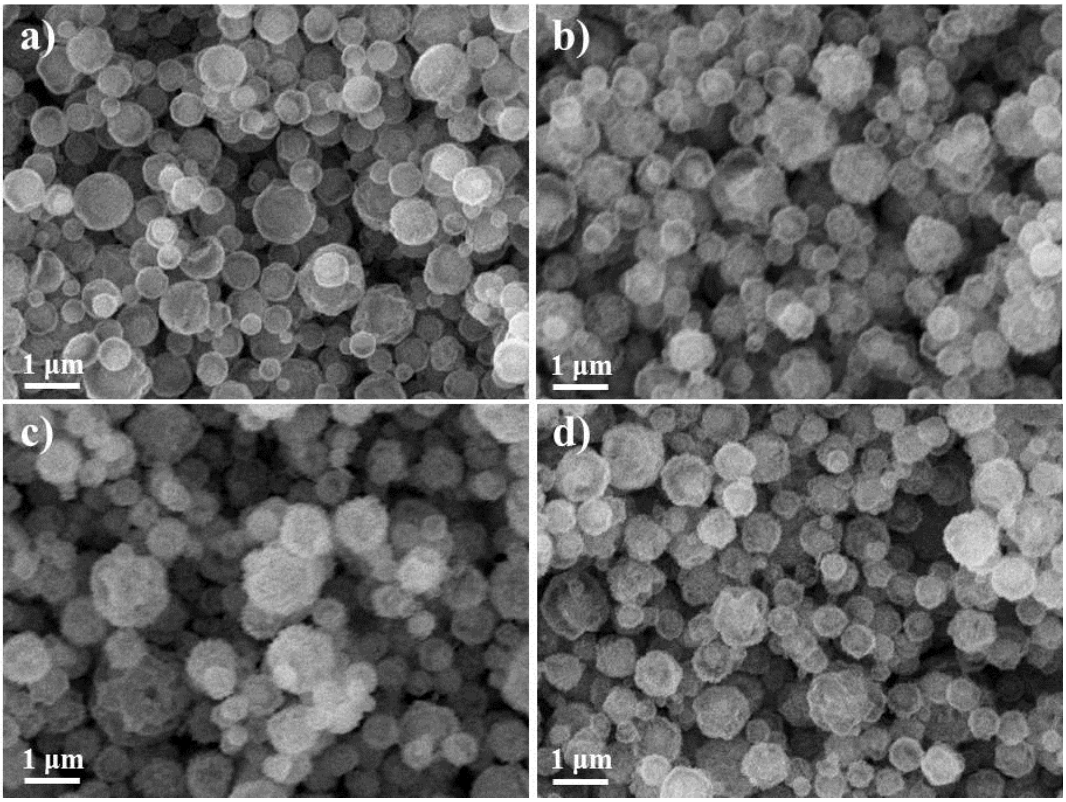


**Fig. S1** SEM images of yolk-shell transition metal oxide powders with 7 to 10 components: a) 7-composite, b) 8-composite, c) 9-composite, and d) 10-composite.

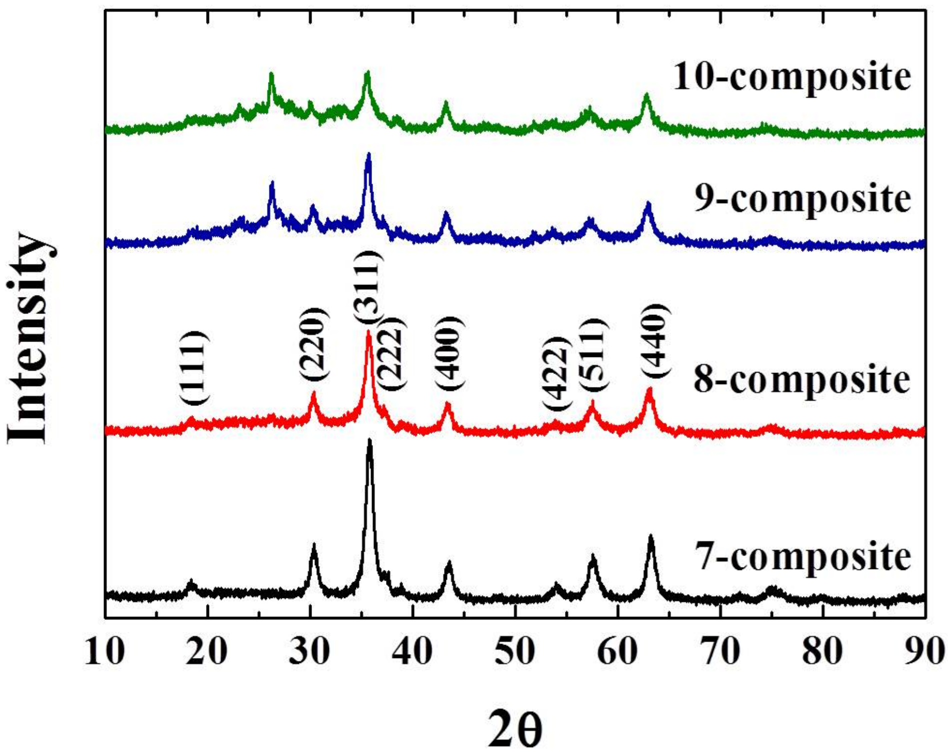


**Fig. S2** XRD patterns of yolk-shell transition metal oxide powders with 7 to 10 components.

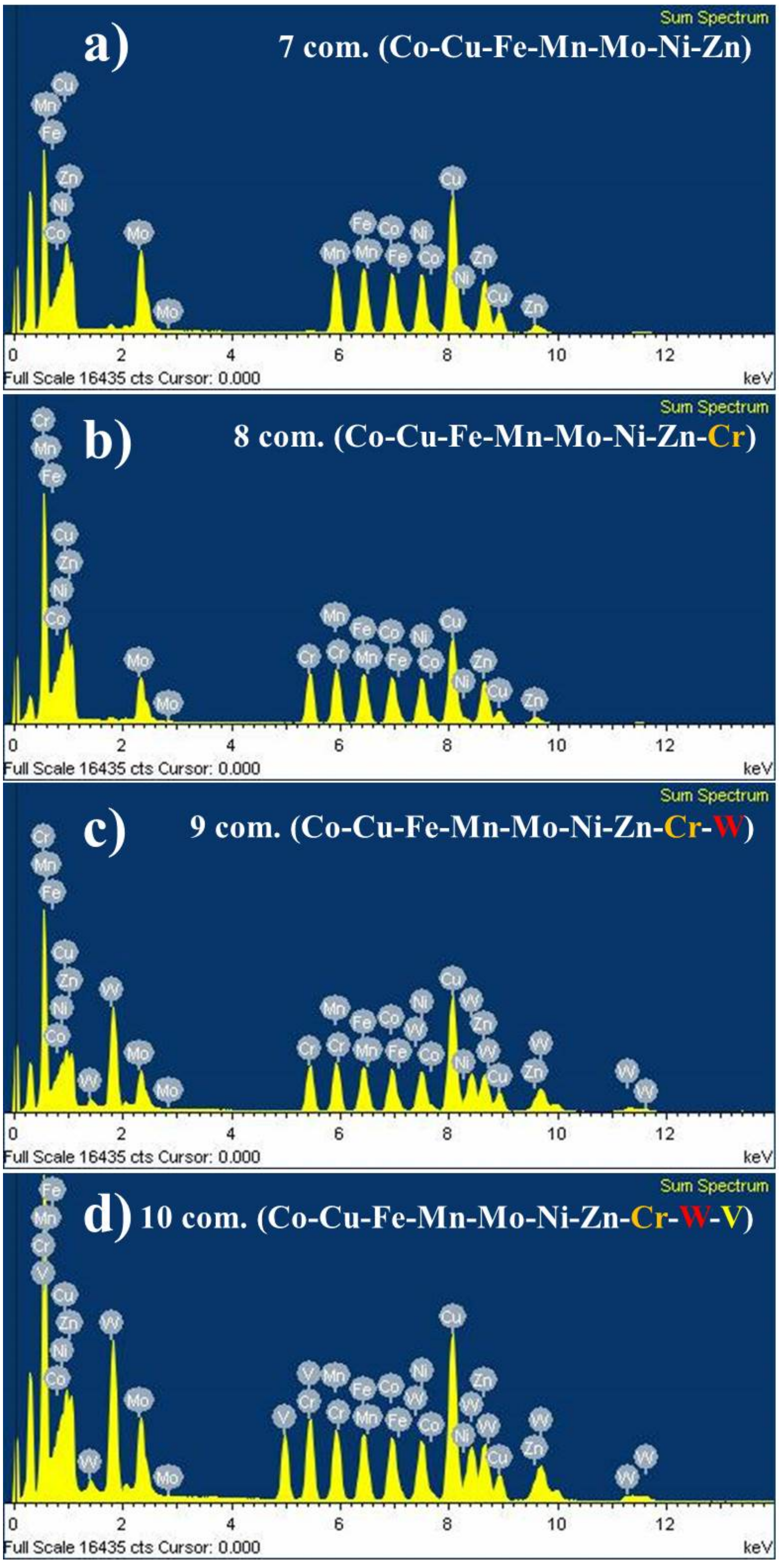


**Fig. S3** Energy dispersive X-ray spectroscopy (EDS) results of the yolk-shell powders with 7, 8, 9, and 10 components.

**Table S1.** Compositions of the yolk-shell powders with 7, 8, 9, and 10 components evaluated by Energy dispersive X-ray spectroscopy (EDS) analysis.

| **Element** | **7-composite atomic %** | **8-composite atomic %** | **9-composite atomic %** | **10-composite atomic %** |
|---|---|---|---|---|
| **Co** | 10.89 | 10.69 | 8.85 | 7.36 |
| **Zn** | 10.91 | 20.02 | 9.08 | 7.44 |
| **Fe** | 10.99 | 10.70 | 8.79 | 7.33 |
| **Mn** | 10.92 | 10.31 | 8.94 | 7.28 |
| **Mo** | 16.69 | 15.80 | 8.45 | 10.40 |
| **Ni** | 11.17 | 10.80 | 8.80 | 7.32 |
| **Cu** | 28.43 | 20.02 | 27.72 | 29.96 |
| **Cr** | - | 10.86 | 8.85 | 7.51 |
| **W** | - | - | 10.34 | 8.06 |
| **V** | - | - | - | 7.34 |

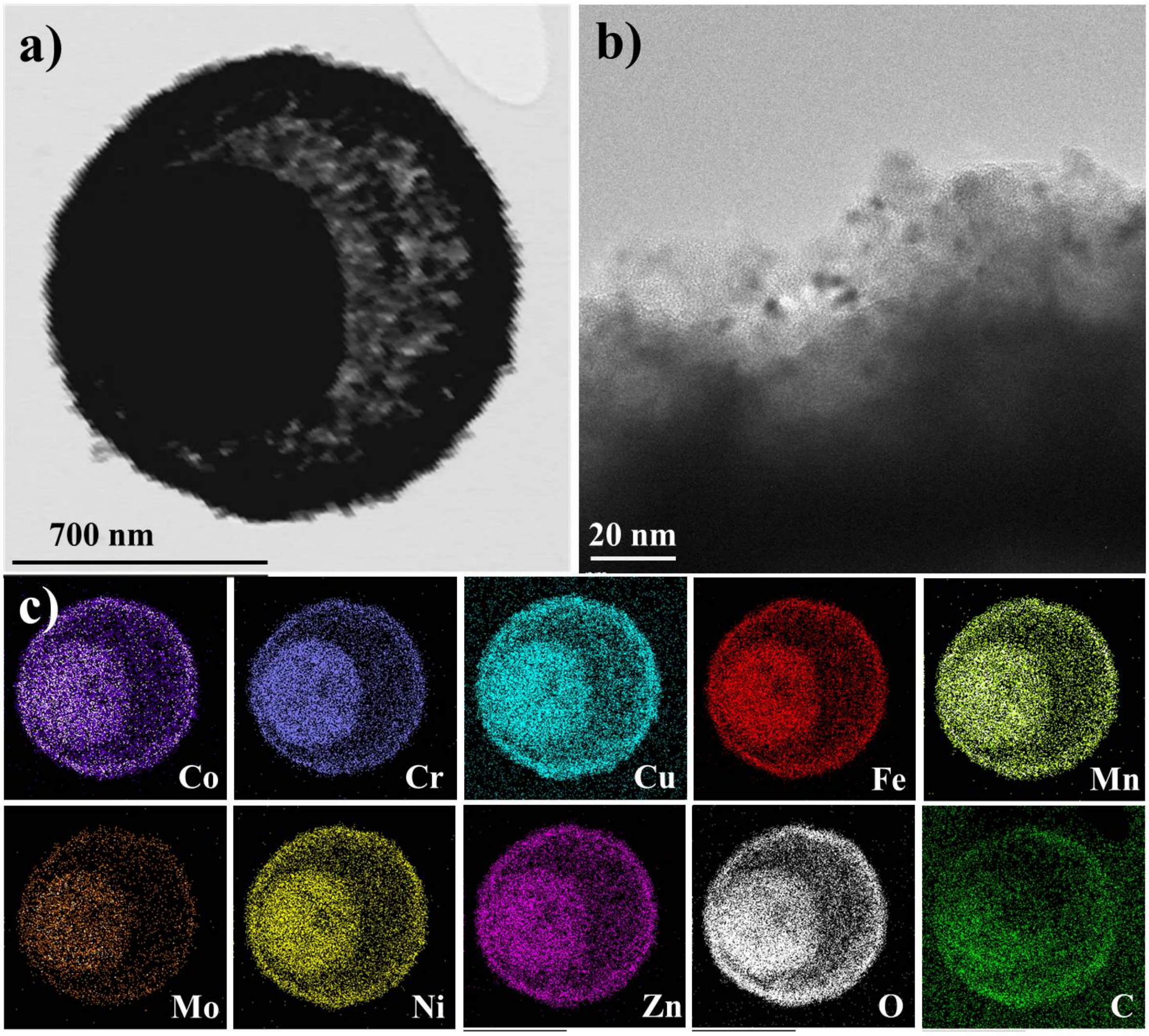


**Fig. S4** TEM and elemental mapping images of the 8-composite material obtained after 300 cycles: a) TEM image, b) high resolution TEM image, and c) elemental mapping images.

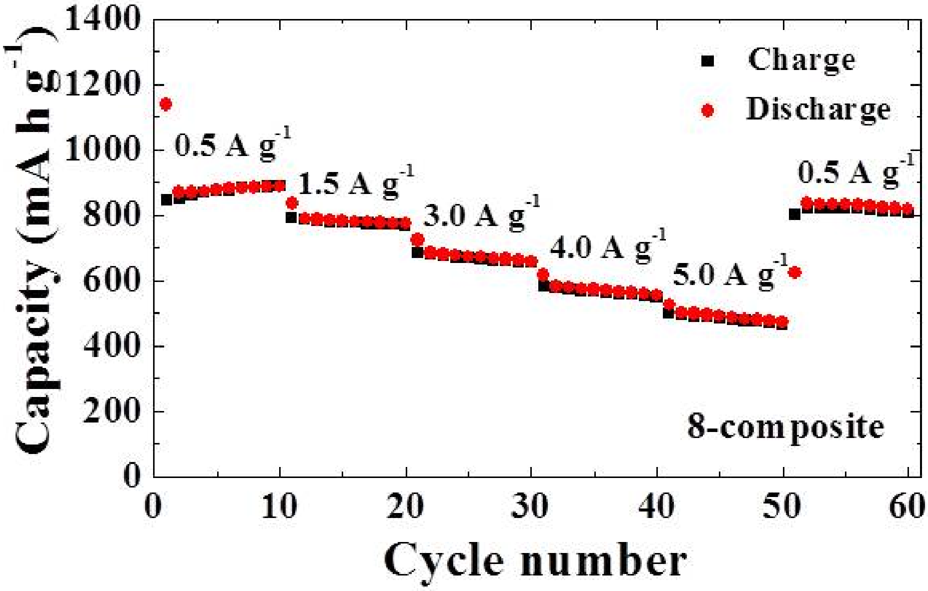


**Fig. S5** Rate performance of 8-composite at a various current densities.

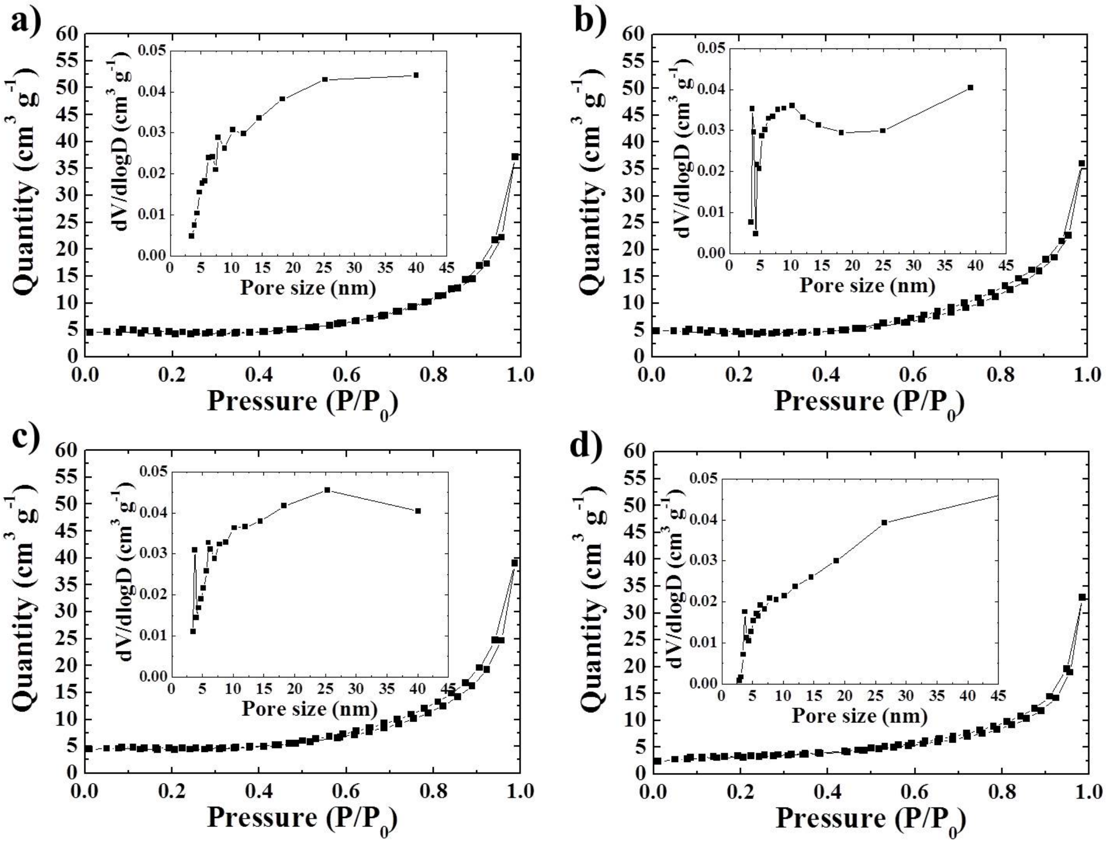


**Fig. S6** $N_2$ adsorption/desorption isotherms and pore size distributions of yolk-shell transition metal oxide powders with 7 to 10 components.

**Table S2.** List of metal precursors for preparing the yolk-shell powders with multicomponent.

| Elemental | Salt name | Formula | Company | Purity |
|---|---|---|---|---|
| **Co** | Cobalt nitrate hexahydrate | $Co(NO_3)_2{\cdot}6H_2O$ | Junsei | 97% |
| **Cu** | Copper nitrate trihydrate | $Cu(NO_3)_2{\cdot}3H_2O$ | Junsei | 99% |
| **Fe** | Iron nitrate nonahydrate | $Fe(NO_3)_3{\cdot}9H_2O$ | Samchun | 98% |
| **Mn** | Manganese nitrate hexahydrate | $Mn(NO_3)_2{\cdot}6H_2O$ | Junsei | 97% |
| **Mo** | Ammonium molybdate | $(NH_4)_6Mo_7O_{24}{\cdot}4H_2O$ | Samchun | 98% |
| **Ni** | Nickel nitrate hexahydrate | $Ni(NO_3)_2{\cdot}6H_2O$ | Junsei | 97% |
| **Zn** | Zinc nitrate hexahydrate | $Zn(NO_3)_2{\cdot}6H_2O$ | Samchun | 98% |
| **Cr** | Chromium nitrate nonahydrate | $Cr(NO_3)_2{\cdot}9H_2O$ | Junsei | 98% |
| **W** | Ammonium tungstate hydrate | $(NH_4)_{10}H_2(W_2O_7)_6{\cdot}x\ H_2O$ | Sigma-Aldrich | 99% |
| **V** | Vanadium oxide | $V_2O_5$ | Junsei | 99% |